

Supplementary information for: Entropy-enthalpy compensation in Ti-V-Mn-Cr BCC alloys used as hydrogen storage materials.

Pressure-Composition-Isotherms (PCI) measurements: Accompanying the main text, the supplementary material presents four figures that correspond to the figures in the article.

In the main text of our article, we present the Pressure-Composition-Temperature (PCT) desorption curves of the $\text{Ti}_{30}\text{V}_{60}\text{Mn}_{(10-x)}\text{Cr}_x$ ($x=0, 3.3, 6.6, \text{ and } 10$) + 4 wt.% Zr alloy (**Figure 1(a)-4(a)**), aligned at their inflection points (i.e., middle of the plateau) to facilitate a direct comparison of the plateau regions. However, to provide a complete view of the data and to maintain transparency of our methodological approach, this supplementary document will include the original PCT curves without any vertical alignment. This will allow interested readers to observe the original starting points of each desorption curve at their actual high-pressure origins, as recorded during the experiments.

The article's experimental section outlines the hydrogenation process we administered prior to recording each PCT desorption curve. Notably, we did not perform the absorption part of the PCI at temperatures ranging from 398 to 498 K due to high hysteresis, which makes the absorption pressure at these temperatures above the limit of our apparatus. Therefore, as our study was solely focused on desorption, all presented curves originate from the same high-pressure point.

- Figure S1 shows the PCI desorption curves of $\text{Ti}_{30}\text{V}_{60}\text{Mn}_{10}$ + 4 wt.% Zr alloy and the corresponding Van't Hoff plot. In the paper, the inflection point is situated at 0.7 wt.%.

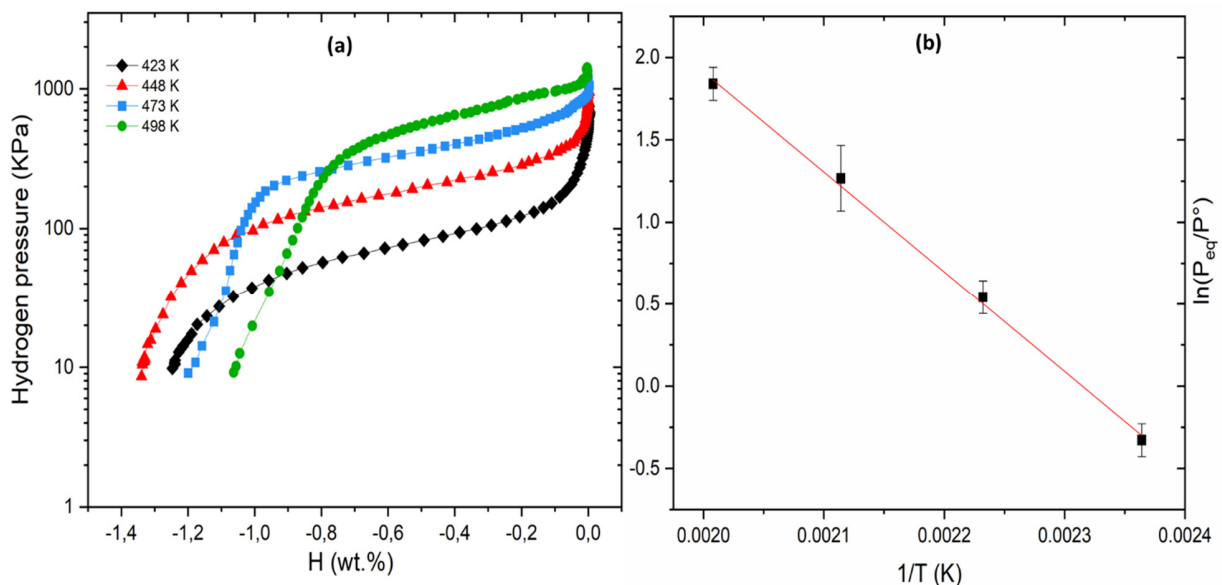


Figure S1: PCI desorption curves at 423, 448, 473 and 498 K (a) and Van't Hoff plot of $\text{Ti}_{30}\text{V}_{60}\text{Mn}_{10}$ + 4 wt.% Zr alloy (b).

- Figure S2 illustrates the PCI desorption curves of $\text{Ti}_{30}\text{V}_{60}\text{Mn}_{6.6}\text{Cr}_{3.3} + 4 \text{ wt.}\% \text{ Zr}$ and the corresponding Van't Hoff plot. In the paper, the inflection point is placed at 0.75 wt.%.

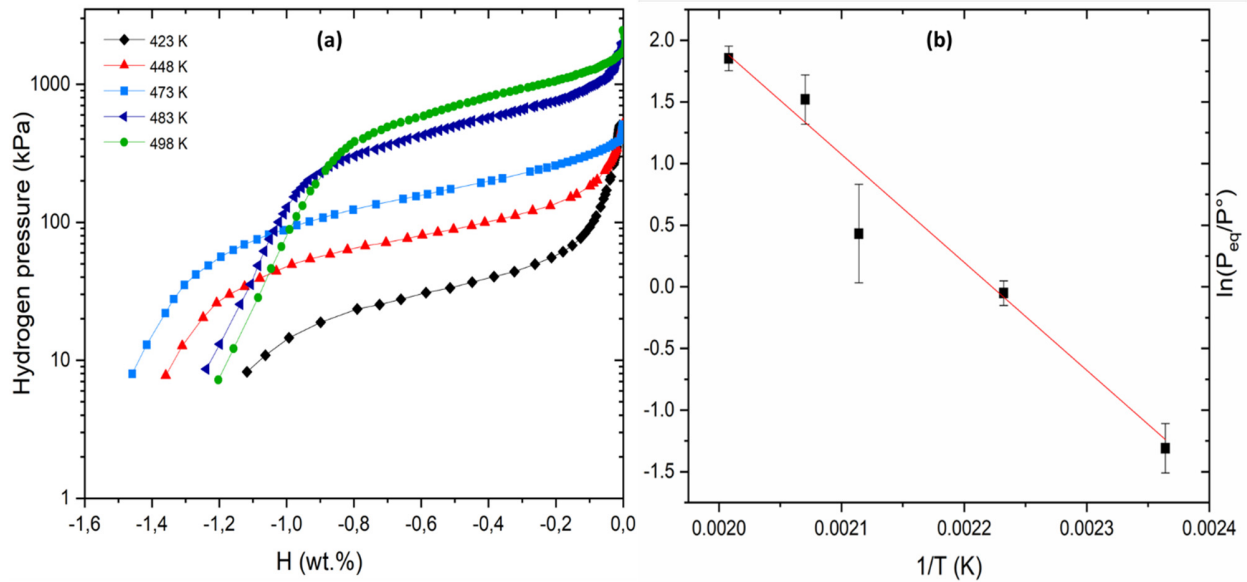


Figure S2: PCI desorption curves at 423, 448, 473, 483 and 498 K (a) and Van't Hoff plot of $\text{Ti}_{30}\text{V}_{60}\text{Mn}_{6.6}\text{Cr}_{3.3} + 4 \text{ wt.}\% \text{ Zr}$ alloy (b).

- Figure S3 represents the PCI desorption curves of $\text{Ti}_{30}\text{V}_{60}\text{Mn}_{3.3}\text{Cr}_{6.6} + 4 \text{ wt.}\% \text{ Zr}$ and its Van't Hoff plot. In the paper, the inflection point is situated at 0.8 wt.%.

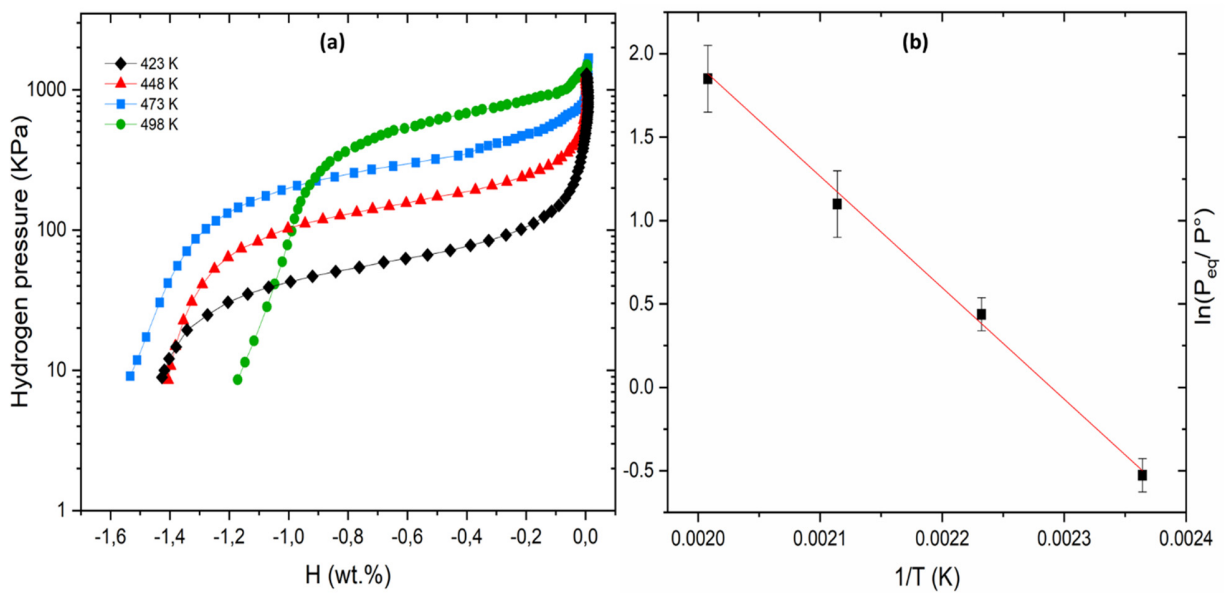


Figure S3: PCI desorption at 423, 448, 473 and 498 K (a) and Van't Hoff plot of $\text{Ti}_{30}\text{V}_{60}\text{Mn}_{3.3}\text{Cr}_{6.6} + 4 \text{ wt.}\% \text{ Zr}$ alloy (b).

- Figure S4 presents the PCI desorption curves of $\text{Ti}_{30}\text{V}_{60}\text{Cr}_{10} + 4 \text{ wt.}\% \text{ Zr}$ alloy and the corresponding Van't Hoff plot. In the paper, the inflection point is placed at 0.7 wt.%.

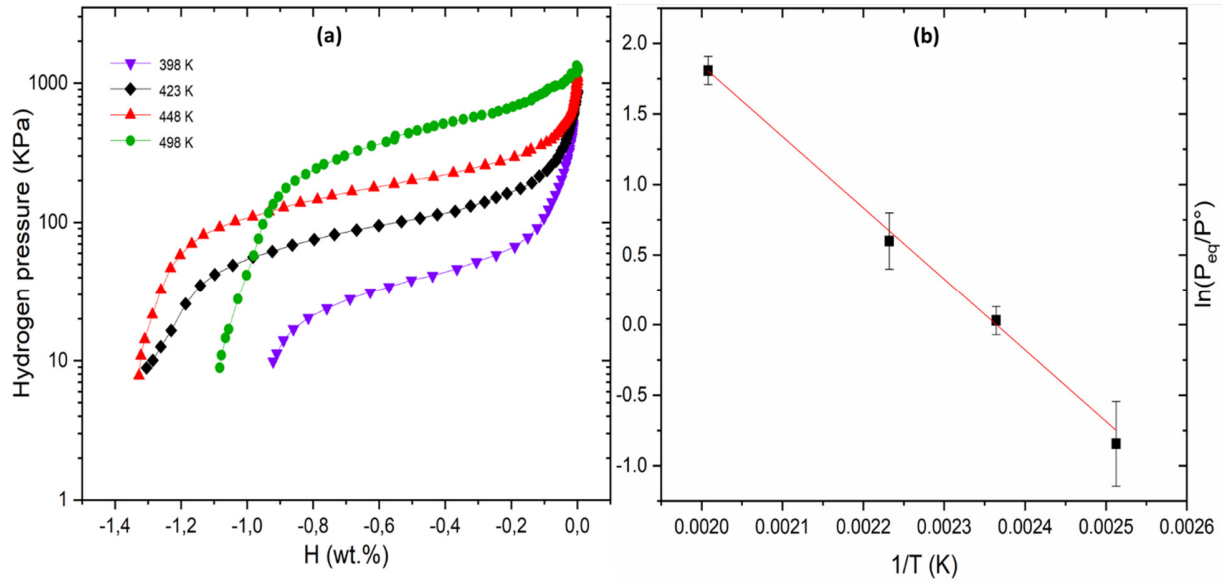


Figure S4: PCI desorption at 398, 423, 448 and 498 K (a) and Van't Hoff plot of $\text{Ti}_{30}\text{V}_{60}\text{Cr}_{10} + 4 \text{ wt.}\% \text{ Zr}$ alloy (b).